Predictive DTC algorithm for Induction Machines using Sliding Horizon Prediction

Johnny Rengifo and José Aller
Departamento de Conversión y Transporte de Energía
Universidad Simón Bolívar
jwrengifo@usb.ve/jaller@usb.ve

Alberto Berzoy and José Restrepo
Departamento de Electrónica y Circuitos
Universidad Simón Bolívar
aberzoya@usb.ve/restrepo@usb.ve

***Abstract*—This paper presents a predictive direct torque control PDTC algorithm for induction machine drives including a Sliding Horizon Prediction (SH-PDTC). The selected strategy for the SH-PDTC algorithm was to keep the motor torque and stator flux-linkage within predefined hysteresis bounds while reducing inverter switching losses. The proposed SH-PDTC algorithm shows better performance in torque and stator flux-linkage control in comparison with classical PDTC, without increasing power losses in the inverter. A sensitivity analysis allows to evaluate algorithm performance under parameter uncertainty, and the results show that SH-PDTC keeps torque ripple performance. The paper includes a simulation to verify the PDTC and SH-PDTC algorithms controlling an induction machine, with a standard two level inverter.**

***Index Terms*—Induction machine, DTC, Predictive control, Sliding horizon prediction, Switching losses.**

I. Introduction

The conventional Direct Torque Control (DTC) algorithm is a tool widely used in industrial control systems. This technique is robust to uncertainty in model parameters of the electromechanical converters [1]. The main drawback of DTC is the large amount of current and torque ripple. A reduction in the state variable's ripple is possible with an algorithm employing a model of the system. This model helps to predict the state variables evolution when using DTC (Predictive DTC (PDTC)), and allows selecting the control action that minimizes a given cost function. [2], [3], [4], [5]

This paper proposes a control scheme based on predictive DTC, including a finite sliding horizon prediction (SH-PDTC). The main idea of the proposed SH-PDTC algorithm is the use of multistep predictions forward in time. A cost function selects the optimum trajectory in the proposed horizon, and the corresponding voltage vector of this optimum trajectory is applied by the inverter. The control procedure starts again after moving the control horizon a step in future.

The cost function used to improve the PDTC considers the losses in the converter bridged only for the possible solutions satisfying the torque and flux-linkage constrains. The simulations show that the proposed SHP-DTC algorithm reduces torque ripple to about 70% of classical DTC. That is, the proposed algorithm minimizes commutations in the inverter bridge while achieving values of torque and flux-linkage closer to the reference than in classical DTC. Also, a sensitivity study to variation in the machine's model parameters shows the adaptability of the algorithm.

The simulation shows a comparison of PDTC and SHP-PDTC for induction motor controllers. Both cases use the same torque and flux-linkage references. The simulation employs an evaluation of the bridge converter losses for use by the cost function. Finally, the introduction of an indicator for torque ripple provides a measurement for comparing the classical and the proposed control algorithms.

II. Induction machine model

The space vector model of the induction machine in the fixed stator reference frame $\alpha\beta$, can be represented as [6],

$$p\vec{i}_s = \frac{L_r}{\Delta}\vec{v}_s - \frac{L_sR_r + L_rR_s}{\Delta}\vec{i}_s + \frac{R_r}{\Delta}\vec{\lambda}_s + \cdots$$
$$\cdots + jn_p\omega_m\vec{i}_s - jn_p\omega_m\frac{L_r}{\Delta}\vec{\lambda}_s \quad (1)$$

$$p\vec{\lambda}_s = \vec{v}_s - R_s\vec{i}_s \quad (2)$$

$$p\omega_m = \frac{1}{J}\left(n_p\vec{\lambda}_s \times \vec{i}_s - T_m\right) \quad (3)$$

978-1-4799-2507-0/14/$31.00 ©2014 IEEE

where, $p = {}^{d}/_{dt}$, $\vec{i}_s$ is the stator current space vector, $\vec{\lambda}_s$ is the stator flux-linkage space vector and $\vec{v}_s$ is the stator voltage space vector. The parameters required by this model are the stator resistance R_s, the stator inductance L_s, the rotor resistance R_r, the rotor inductance L_r, the coupling stator-rotor inductance L_{sr}, Δ is defined as $\Delta \equiv L_s L_r - L_{sr}^2$, the number of pole pairs n_p and the moment of inertia J. T_m is the mechanical load torque and ω_m is the mechanical angular speed. The space vector coordinate transformation $\alpha\beta$ used in this paper is,

$$\vec{x} = \sqrt{\frac{2}{3}}\left(x_a + x_b e^{j\frac{2\pi}{3}} + x_c e^{j\frac{4\pi}{3}}\right) = x_\alpha + j x_\beta \tag{4}$$

III. Sliding horizon predictive direct torque control

A. Control problem

The objective of the SH-PDTC is to keep the electric torque and the amplitude of the stator flux-linkage space vector within bounds around their references, reducing the power losses of the converter over a prediction horizon (N). N is the number of control steps in time used for the prediction. The torque reference is set either by the user or by an additional speed control. The flux-linkage reference is set by the user, normally at rated value or using a flux function in the weakening range.

The algorithm establishes the control's actions through a three level comparator; the separation of the control boundaries is set by the user according the required system performance. The following expression, (5), shows the possible outputs for comparators S_T and S_λ,

$$S_y = \begin{cases} 1 & y > y_{max} \\ 0 & y_{min} \le y \le y_{max} \\ -1 & y < y_{min} \end{cases} \tag{5}$$

where y refers to T_e or $\left|\vec{\lambda}_s\right|$. Lower and upper bounds are defined by the following expressions,

$$y_{max} = y_{ref} + \frac{HB_y}{2} \;\; ; \;\; y_{min} = y_{ref} + \frac{HB_y}{2} \tag{6}$$

where HB_y refers to the hysteresis bands of each controlled variable. The output of each comparator points to increasing, decreasing or keeping the electric torque or the magnitude of stator flux-linkage. From the induction machine model (1)-(3), it is possible to deduce expressions for the time derivative of the torque and stator flux-linkage magnitude as a function of the stator current vector $\vec{i}_s$, the flux-linkage vector $\vec{\lambda}_s$, the mechanical angular speed ω_m and the stator voltage vector $\vec{v}_s$,

$$pT_e = \Re e\left\{\vec{v}_s^{\,*}\left(\vec{i}_s - \frac{L_r}{\Delta}\vec{\lambda}_s\right)\right\} - \frac{R_r L_s + R_s L_r}{\Delta} T_e + \cdots$$
$$\cdots + \omega_m \Re e\left\{\vec{i}_s \vec{\lambda}_s\right\} - \frac{\omega_m L_r}{\Delta}\left|\vec{\lambda}_s\right|^2 \tag{7}$$

$$p\left|\vec{\lambda}_s\right| = \frac{1}{\left|\vec{\lambda}_s\right|}\left(\Re e\left\{\vec{\lambda}_s^{\,*}\left(\vec{v}_s - R_s\vec{i}_s\right)\right\}\right) \tag{8}$$

where the superscript * stands for the complex conjugated.

The time derivatives for the stator flux-linkage and electric torque shown in (7) and (8) allow to assess the voltage vector available in the inverter to increase, decrease or maintain the controlled variable.

Each voltage vector available in the inverter is used to evaluate derivatives of the electric torque and the magnitude of stator flux-linkage. The voltage vectors that satisfy the control's actions are candidates to be fed to the electrical machine. The candidate voltage vectors form the subset $\mathscr{U}_c$. $\mathscr{U}_c = \left\{\vec{v}_s^{(1)}, \vec{v}_s^{(2)}, \ldots, \vec{v}_s^{(d)}\right\}$, where d is the number of voltage vectors satisfying the control actions.

In particular, when the control action requires to keep a controlled variable inside a given hysteresis band, the best solution is the space voltage vector that nullifies or minimizes pT_e or $p\left|\vec{\lambda}_s\right|$. However, for the finite set of voltage vectors available in the converter, this solution is difficult to achieve. Therefore, it is necessary to define a tolerance band for pT_e and $p\left|\vec{\lambda}_s\right|$. The controlled variables can move inside this band. These tolerance regions were defined as Tol_T for the electric torque, and as Tol_λ for the stator flux-linkage.

The algorithm in this step chooses the candidates set satisfying the control actions and then estimates the response of the induction machine by solving the equation system presented in (1) - (3). To estimate the state variables one step ahead, the mechanical speed is set as constant, due to the slow variation of the mechanical speed in comparison with electric variables. Euler's method is used to estimate the new value of the state variables,

$$\mathbf{x}_{k+1} = \mathbf{x}_k + T_s p\mathbf{x}_k \tag{9}$$

where, $\mathbf{x}_k^{(d)} = \left[\vec{i}_{s_k} \quad \vec{\lambda}_{s_k}\right]^t$, k actual control instant and T_s is the integration step.

The controlled variables $\mathbf{y}_{k+1}^{(d)} = \left[T_{e_{k+1}} \quad \left|\vec{\lambda}_{s_{k+1}}\right|\right]^t$ are calculated in the predicted state $\mathbf{x}_{k+1}^{(d)}$. For each space voltage vector that belongs to $\mathscr{U}_{c_k}$, the corresponding predicted controlled output $\mathbf{y}_{k+1}^{(d)}$ is obtained. For each state $\mathbf{x}_{k+1}^{(d)}$ the algorithm

is repeated and the new output $\mathbf{y}_{k+2}^{(d)}$ is calculated. The outputs $\mathbf{y}_{k+1}^{(d)}$ and $\mathbf{y}_{k+2}^{(d)}$, corresponding to each element in $\mathscr{U}_{c_k}$, for a trajectory path $Y^{(d)}$. Each path has N elements, one for each step in the prediction horizon used. These paths $Y^{(d)} = \left\{\mathbf{y}_{k+1}^{(d)}, \mathbf{y}_{k+2}^{(d)}, \ldots, \mathbf{y}_{k+N}^{(d)}\right\}$ will be used to evaluate the cost function.

B. Energy loss estimation

In [7], [8] Rajapakse et. al. presented methods to estimate the power losses in an IGBT. Those methods use the characteristic dynamic wave forms of voltage, current, and datasheet parameters to calculate energy losses. The IGBT's power losses can be classified in conduction losses, turn-on switching losses, turn-off switching losses, and off-state blocking losses. In the first case, conduction losses are calculated as the product of the load current and the saturation voltage. While, the blocking losses are calculated as the product between the leakage current and the blocking voltage. For present day devices, the blocking power losses are negligible [7]. Finally, the switching losses are divided in: diode's turn-on and turn-off, and IGBT's turn-on and turn-off.

As explained in [7], [8], the switching power losses depend on the device voltage and current transient characteristics, therefore the proposed control algorithm proposed uses an approximation to quantify the switching energy losses during the operation of an IGBT. Those wave forms are shown in figure 1. The cost function target is to penalize control actions that imply high power losses.

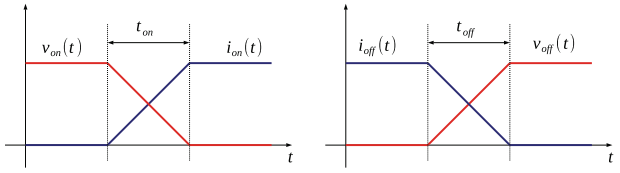

(a) Turn-on (b) Turn-off

Figure 1: IGBT switching voltage and current approximation for power losses estimation

C. Cost function

For each space voltage vector present in $\mathscr{U}_c$ a new state $\mathbf{x}_{k+1}^{(d)}$ is estimated, including the corresponding losses in the converter. This process is repeated many times as indicated by the prediction horizon (N). The cost function summarizes the switching energy losses ($E_{sw-losses}$) produced in each trajectory over the prediction horizon, and the voltage vector selected will be the one in the subset that totalize the minimum energy losses.

$$D_k = \arg\min_{d_k} \left\{ \sum_{m=1}^{N} \left(\zeta_1 E_{sw-losses}^{(d)} + \zeta_2 \left| \mathbf{y_{ref}} - \mathbf{y}_{k+m}^{(d)} \right| \right) \right\} \quad (10)$$

where D_k is the index associated to the space voltage $\mathscr{U}_c$, that minimizing the cost function set 10 for a prediction horizon N steps after the current time k. ζ_1 and $\zeta_2$are positive weights.

D. Non feasible states

Selection of the candidates voltage vectors can result in a null subset, i.e., there are not any voltage space vectors able to satisfy the control constrains over the controlled state variables. These cases are defined as non feasible states. The proposed strategy to handle it, consist in selecting the voltage space vector that produces the smallest deviation of the controlled variables respect their references. The estimation of the controlled variables is made with a first order approximation over a prediction horizon equal to one,

$$T_{e_{k+1}} = T_{e_k} + pT_e|_k T_s \,;\, \left|\vec{\lambda}_{s_{k+1}}\right| = \left|\vec{\lambda}_{s_k}\right| + p\left|\vec{\lambda}_s\right|_k T_s \quad (11)$$

with the electric torque and stator flux-linkage estimated, the cost function is defined as,

$$e_T = T_{ref} - T_{e_{k+1}} \,;\, e_\lambda = \left|\vec{\lambda}_{ref}\right| - \left|\vec{\lambda}_{e_k}\right| \quad (12)$$

$$\psi = \rho_1 e_T^2 + \rho_1 e_\lambda^2 \quad (13)$$

where, ρ_1 and ρ_2 are positives weights.

The voltage space vector selected is the one that minimize the cost function (13).

The proposed algorithm SH-PDTC was implemented for an induction machine using a three phase inverter. The motor nameplate information and parameters are presented in table I. The machine's model parameters are expressed in per unit, and the rated values were taken as bases. The study case used to evaluate the SH-PDTC performance was an start-up with a constant reference of the angular speed $\omega_{ref} = 1\,\text{pu}$. The torque reference was obtained from a PI controlled with $k_p = 15\,^{Nms}/_{\text{rad}}$ and $k_p = 1\,^{Nms^2}/_{\text{rad}^2}$. Finally, a load step of $T_m = 0.4$ pu occurs at $t = 1.5\,\text{s}$. The control sampling frequency was 10 kHz. The set of hysteresis bounds was $HB_T = 0.12$ pu, $HB_\lambda = 0.05$ pu, $Tol_T = 1.6$ pu and $Tol_\lambda = 0.45$ pu.

Table I: Induction machine name plate and parameters

V_n[V]	I_n[A]	P_n [hp]	$\cos\varphi_n$	n_n[rpm]	
230	16.58	6.17	0.82	1720	
R_e[pu]	L_{σ_e}[pu]	R_r[pu]	L_{σ_r}[pu]	L_{er}[pu]	H [ms]
0,047	0,0664	0,0402	0,0664	2,3768	252

IV. Simulations results

To compare the performance of the proposed strategy SH-PDTC, the algorithm representing the PDTC was the one presented in [2].

This paper proposes a variable σ_T to quantify the torque ripple. The aim is to measure the average deviation of the torque with respect to its reference over a period of time,

$$\sigma_T = 100 \times \frac{1}{N_i} \sum_{k=1}^{N_i} \frac{1}{T_{ref_k}} \sqrt{\left(T_{ref_k} - T_{e_k}\right)^2} \qquad (14)$$

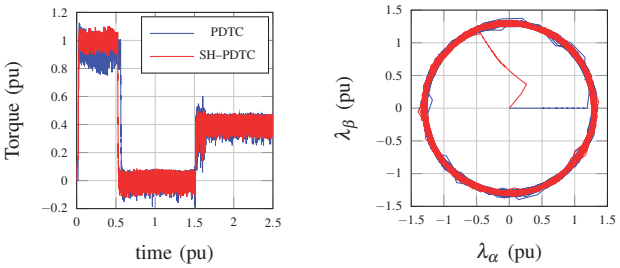

(a) Electric torque (b) Stator flux-linkage

Figure 2: PDTC and SH-PDTC simulation results

Table II: Electric torque ripple

	DTC	PDTC	SH-PDTC
σ_T (%)	32.70	15.01	9.46
Switch. losses (pu)	0.0072	0.0071	0.0070

Figure 2 shows the electric torque response and the stator flux-linkage locus using both strategies. Table II shows the torque ripple results. This results were calculated using (14) during steady state operation. Additionally, Classic DTC torque ripple was included in the analysis. The SH-PDTC reduces the torque ripple in about 37%, with respect to PDTC, using $N = 2$. The switching losses of the strategies were determined using the method presented in [8]. The IGBT parameters used in the simulation were [9].

A. Sensitivity analysis

The proposed predictive algorithm requires the machine parameters, and any method used to measure or estimate these parameters have some degree of uncertainty. To evaluate the performance of SH-PDTC some of the parameters were changed over uncertainty limits ($\pm 30\%$). These parameters are rotor resistance R_r, dispersion inductance ($L_\sigma = L_{\sigma_s} + L_{\sigma_r}$) and the coupling stator-rotor inductance L_{sr}. The maximum torque ripple is 11.2% and without the uncertainty 9.46%.

V. Conclusions

The SH-PDTC method can reduce the electric torque ripple keeping constant the switching power losses. The algorithm was verified with simulations using a horizon prediction $N = 2$. The proposed method is robust to parameters uncertainties below $\pm 30\%$. The next step will be to increase the horizon prediction and the algorithm's experimental validation.

VI. Acknowledgment

This work was supported by FONACIT-Venezuela under project Number 201100348.

References

[1] I. Takahashi and T. Noguchi, "A new Quick-Response and High-Efficiency control strategy of an induction motor," *IEEE Transactions on Industry Applications*, vol. IA-22, pp. 820–827, Sept. 1986.

[2] G. Escobar, A. M. Stankovic, E. Galvan, J. M. Carrasco, and R. Ortega, "A family of switching control strategies for the reduction of torque ripple in DTC," *IEEE Transactions on Control Systems Technology*, vol. 11, pp. 933– 939, Nov. 2003.

[3] A. Linder and R. Kennel, "Direct model predictive control - a new direct predictive control strategy for electrical drives," in *2005 European Conference on Power Electronics and Applications*, pp. 10 pp.–P.10, IEEE.

[4] T. Geyer, G. Papafotiou, and M. Morari, "Model predictive direct torque Control-Part i: Concept, algorithm, and analysis," *IEEE Transactions on Industrial Electronics*, vol. 56, pp. 1894–1905, June 2009.

[5] J. Beerten, J. Verveckken, and J. Driesen, "Predictive direct torque control for flux and torque ripple reduction," *Industrial Electronics, IEEE Transactions on*, vol. 57, no. 1, pp. 404–412, 2010.

[6] A. Trzynadlowski, *The Field Orientation Principle in Control of Induction Motors*. Springer, Dec. 1993.

[7] A. Rajapakse, A. Gole, and P. Wilson, "Electromagnetic transients simulation models for accurate representation of switching losses and thermal performance in power electronic systems," *Power Delivery, IEEE Transactions on*, vol. 20, pp. 319–327, Nov. 2005.

[8] A. Rajapakse, A. Gole, and R. Jayasinghe, "An improved representation of facts controller semiconductor losses in emtp-type programs using accurate loss-power injection into network solution," *Power Delivery, IEEE Transactions on*, vol. 24, pp. 381–389, Jan. 2009.

[9] F. SEMICONDUCTOR, "FP7G50US60 transfer molded type IGBT module," 2008.